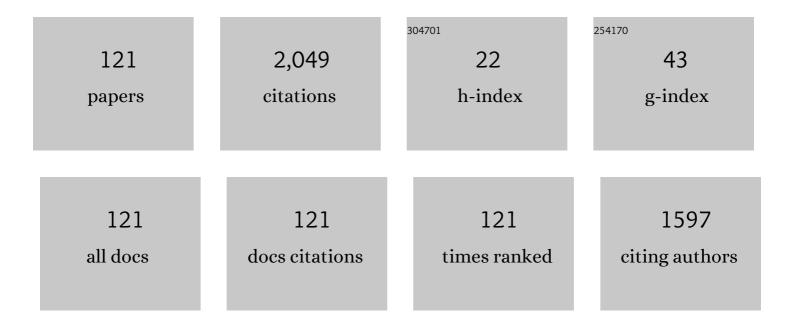
List of Publications by Year in descending order

Source: https://exaly.com/author-pdf/2434592/publications.pdf Version: 2024-02-01



#	Article	IF	CITATIONS
1	Dielectric Properties of (Ba, Sr)TiO3Thin Films Deposited by RF Sputtering. Japanese Journal of Applied Physics, 1993, 32, 4126-4130.	1.5	233
2	50-Gb/s ring-resonator-based silicon modulator. Optics Express, 2013, 21, 11869.	3.4	165
3	Dielectric Properties of(BaxSr1-x)TiO3Thin Films Prepared by RF Sputtering for Dynamic Random Access Memory Application. Japanese Journal of Applied Physics, 1994, 33, 5187-5191.	1.5	110
4	First Demonstration of Athermal Silicon Optical Interposers With Quantum Dot Lasers Operating up to 125 °C. Journal of Lightwave Technology, 2015, 33, 1223-1229.	4.6	106
5	Dielectric Relaxation of (Ba, Sr) TiO3 Thin Films. Japanese Journal of Applied Physics, 1995, 34, 5478-5482.	1.5	87
6	Comparative Studies on Oxygen Diffusion Coefficients for Amorphous and Î <sup>3</sup> -Al2O3Films using18O Isotope. Japanese Journal of Applied Physics, 2003, 42, 7205-7208.	1.5	79
7	A 300-mm Silicon Photonics Platform for Large-Scale Device Integration. IEEE Journal of Selected Topics in Quantum Electronics, 2018, 24, 1-15.	2.9	74
8	Low-loss silicon wire waveguides for optical integrated circuits. MRS Communications, 2016, 6, 9-15.	1.8	70
9	Thermal Stability of a Thin HfO2/Ultrathin SiO2/Si Structure: Interfacial Si Oxidation and Silicidation. Japanese Journal of Applied Physics, 2003, 42, L138-L140.	1.5	66
10	Graph-theoretical Formula for Ring Currents Induced in a Polycyclic Conjugated System. Bulletin of the Chemical Society of Japan, 1983, 56, 1853-1854.	3.2	65
11	125-Gb/s operation with 029-V·cm V_πL using silicon Mach-Zehnder modulator based-on forward-biased pin diode. Optics Express, 2012, 20, 2911.	3.4	62
12	Low-loss, flat-topped and spectrally uniform silicon-nanowire-based 5th-order CROW fabricated by ArF-immersion lithography process on a 300-mm SOI wafer. Optics Express, 2013, 21, 30163.	3.4	60
13	Demonstration of 125-Gbps optical interconnects integrated with lasers, optical splitters, optical modulators and photodetectors on a single silicon substrate. Optics Express, 2012, 20, B256.	3.4	53
14	Si-nanowire-based multistage delayed Mach–Zehnder interferometer optical MUX/DeMUX fabricated by an ArF-immersion lithography process on a 300  mm SOI wafer. Optics Letters, 2014, 39, 3702.	3.3	48
15	Compact PIN-Diode-Based Silicon Modulator Using Side-Wall-Grating Waveguide. IEEE Journal of Selected Topics in Quantum Electronics, 2013, 19, 74-84.	2.9	43
16	High-density and wide-bandwidth optical interconnects with silicon optical interposers [Invited]. Photonics Research, 2014, 2, A1.	7.0	40
17	General graph-theoritical formula for the London susceptibility of a cyclic conjugated system with highly degenerate orbitals. Chemical Physics Letters, 1983, 95, 561-563.	2.6	36
18	Si Waveguide-Integrated Metal–Semiconductor–Metal and p–i–n-Type Ge Photodiodes Using Si-Capping Layer. Japanese Journal of Applied Physics, 2013, 52, 04CG10.	1.5	34

#	Article	IF	CITATIONS
19	High-speed and high-efficiency Si optical modulator with MOS junction, using solid-phase crystallization of polycrystalline silicon. Japanese Journal of Applied Physics, 2016, 55, 042202.	1.5	32
20	Si wire array waveguide grating with parallel star coupler configuration fabricated by ArF excimer immersion lithography. Electronics Letters, 2013, 49, 410-412.	1.0	29
21	Void nucleation in thin HfO2 layer on Si. Applied Physics Letters, 2003, 82, 3880-3882.	3.3	28
22	Modeling of gas-phase and surface reactions in liquid-source chemical-vapor deposition of (Ba,Sr)TiO3 films. Journal of Applied Physics, 1999, 86, 1082-1089.	2.5	23
23	Conformal Step Coverage of (Ba,Sr)TiO3Films Prepared by Liquid Source CVD Using Ti(t-BuO)2(DPM)2. Japanese Journal of Applied Physics, 1999, 38, 2205-2209.	1.5	22
24	Effect of Al2O3 capping layer on suppression of interfacial SiO2 growth in HfO2/ultrathin SiO2/Si(001) structure. Applied Physics Letters, 2003, 82, 3442-3444.	3.3	22
25	The impacts of fabrication error in Si wire-waveguides on spectral variation of coupled resonator optical waveguides. Microelectronic Engineering, 2016, 156, 46-49.	2.4	21
26	Dual-Tapered 10-\$mu\$m-Spot-Size Converter with Double Core for Coupling Polarization-Independent Silicon Rib Waveguides to Single-Mode Optical Fibers. Applied Physics Express, 2012, 5, 022202.	2.4	19
27	Advantages of HfAlON gate dielectric film for advanced low power CMOS application. Microelectronic Engineering, 2005, 80, 190-197.	2.4	18
28	Nanometer-scale crystallization of thin HfO2 films studied by HF-chemical etching. Applied Physics Letters, 2005, 86, 212907.	3.3	18
29	Polarization Diversified 16λ Demultiplexer Based on Silicon Wire Delayed Interferometers and Arrayed Waveguide Gratings. Journal of Lightwave Technology, 2020, 38, 2680-2687.	4.6	18
30	A Mass Spectrometric Study of Reaction Mechanisms in Chemical Vapor Deposition of(Ba,Sr)TiO3Films. Japanese Journal of Applied Physics, 1997, 36, 2555-2560.	1.5	17
31	Two-dimensional void growth during thermal decomposition of thinHfO2films on Si. Physical Review B, 2005, 71, .	3.2	17
32	SiO2/Si interfaces on high-index surfaces: Re-evaluation of trap densities and characterization of bonding structures. Applied Physics Letters, 2011, 98, 092906.	3.3	14
33	1.2 Tbps/cm <sup>2</sup> Enabling Silicon Photonics IC Technology Based on 40-nm Generation Platform. Journal of Lightwave Technology, 2018, 36, 4701-4712.	4.6	12
34	Si wire array waveguide grating with stray light reduction scheme fabricated by ArF excimer immersion lithography. Electronics Letters, 2013, 49, 1401-1402.	1.0	11
35	Differential receivers with highly -uniform MSM Germanium photodetectors capped by SiGe layer. Optics Express, 2013, 21, 23295.	3.4	11
36	Influence of Buffer Layers and Barrier Metals on Properties of(Ba,Sr)TiO3Films Prepared by Liquid Source Chemical Vapor Deposition. Japanese Journal of Applied Physics, 1997, 36, 5874-5878.	1.5	10

#	Article	IF	CITATIONS
37	Chemical Vapor Deposition Technology of (Ba,Sr)TiO <sub>3</sub> Thin Films for Gbit-Scale Dynamic Random Access Memories. Materials Research Society Symposia Proceedings, 1998, 541, 3.	0.1	10
38	High-performance optical waveguide devices using 300mm Si photonics platform. Microelectronic Engineering, 2016, 156, 55-58.	2.4	10
39	Improved fabrication process for Ru/BST/Ru capacitor by liquid source chemical vapor deposition. Thin Solid Films, 2002, 409, 8-14.	1.8	9
40	Roles of nitrogen incorporation in HfAlO[sub x](N) gate dielectrics for suppression of boron penetration. Journal of Vacuum Science & Technology an Official Journal of the American Vacuum Society B, Microelectronics Processing and Phenomena, 2004, 22, 2128.	1.6	9
41	Carrier separation analysis for clarifying carrier conduction and degradation mechanisms in high-k stack gate dielectrics. Microelectronics Reliability, 2005, 45, 1041-1050.	1.7	9
42	Mechanism of Gradual Increase of Gate Current in High-K Gate Dielectrics and Its Application to Reliability Assessment. , 2006, , .		9
43	Activation of overexpressed glucagonâ€like peptideâ€l receptor attenuates prostate cancer growth by inhibiting cell cycle progression. Journal of Diabetes Investigation, 2020, 11, 1137-1149.	2.4	9
44	Contribution of Quadruply Degenerate π-Electron Orbitals to London Susceptibility. Bulletin of the Chemical Society of Japan, 1983, 56, 1547-1548.	3.2	8
45	Integration of BST thin film for DRAM fabrication. Integrated Ferroelectrics, 1995, 11, 101-109.	0.7	8
46	High speed and highly efficient Si optical modulator with MOS junction for 1.55 µm and 1.3 µm wavelengths. , 2013, , .		8
47	High-density optical interconnects by using silicon photonics. Proceedings of SPIE, 2014, , .	0.8	8
48	Process control and monitoring in device fabrication for optical interconnection using silicon photonics technology. , 2015, , .		8
49	Study on the effects of the Si capping layer growth conditions on the leakage current of Ge photodetector. Japanese Journal of Applied Physics, 2017, 56, 102201.	1.5	8
50	Post-Integrated Dual-Core Large-End Spot-Size Converter With Si Vertical Taper for Fiber Butt-Coupling to Si-Photonics Chip. Journal of Lightwave Technology, 2018, 36, 4783-4791.	4.6	8
51	Effect of the interfacial SiO2 layer thickness on the dominant carrier type in leakage currents through HfAlOxâ^•SiO2 gate dielectric films. Applied Physics Letters, 2004, 85, 6227-6229.	3.3	7
52	Mach-Zehnder filter using multiple Si waveguide structure sections for width error tolerance. Electronics Letters, 2012, 48, 869.	1.0	7
53	Degradation mechanism of HfAlOXâ^•SiO2 stacked gate dielectrics studied by transient and steady-state leakage current analysis. Journal of Applied Physics, 2005, 97, 074505.	2.5	6
54	Abrupt Lateral-Source Heterostructures with Relaxed/Strained Layers for Ballistic Complementary Metal Oxide Semiconductor Transistors Fabricated by Local O+Ion-Induced Relaxation Technique of Strained Substrates. Japanese Journal of Applied Physics, 2011, 50, 04DC02.	1.5	6

TSUYOSHI HORIKAWA

#	Article	IF	CITATIONS
55	High precision Si waveguide devices designed for 1.31μm and 1.55μm wavelengths on 300mm-SOI. , 2014, , .		6
56	High density optical and electrical interfaces for chip-scale silicon photonic receiver. , 2017, , .		6
57	A 300-mm-wafer silicon photonics technology for ultra-low-energy optical network systems. , 2017, , .		6
58	Decomposition of SiN interlayer during thermal annealing of HfAlOxâ^•SiNâ^•Si(001) structure. Applied Physics Letters, 2004, 84, 5326-5328.	3.3	5
59	Reliability Perspective of High-k Gate Stack Assessed by Temperature Dependence of Dielectric Breakdown. , 2007, , .		5
60	Reflectance Difference Spectroscopy in Vacuum–Ultraviolet Range: Developing Measurement System and Applying to Characterization of SiO2/Si Interfaces. Japanese Journal of Applied Physics, 2010, 49, 022403.	1.5	5
61	Delayed Interferometer Based Si-wire WDM Demultiplexers Fabricated by Phase Controllable and Productive 300-mm Wafer-scale ArF-Immersion Lithography Technology. , 2014, , .		5
62	Demonstration of over 1000-Channel Hybrid Integrated Light Source for Ultra-High Bandwidth Interchip Optical Interconnection. , 2014, , .		5
63	Phase behaviors for silicon-wire multistage delayed interferometric WDM filters across a whole 300-mm silicon-on-insulator wafer. Journal of the Optical Society of America B: Optical Physics, 2020, 37, 1847.	2.1	5
64	<title>High-resolution display using a laser-addressed ferroelectric liquid-crystal light valve</title> . , 1991, , .		4
65	Measurement of Atomic Incorporation Rates and Modeling of Surface Reactions in (Ba, Sr)TiO3Films Prepared by a Liquid Source Chemical Vapor Deposition. Japanese Journal of Applied Physics, 2001, 40, 3435-3441.	1.5	4
66	Demonstration of 12.5-Gbps Optical Interconnects Integrated with Lasers, Optical Splitters, Optical Modulators and Photodetectors on a Single Silicon Substrate. , 2012, , .		4
67	Demonstration of 25-Gbps optical data links on silicon optical interposer using FPGA transceiver. , 2014, , .		4
68	Resonant Wavelength Variation Modelling for Microring Resonators based on Fabrication Deviation Analysis. , 2017, , .		4
69	Study of HfAlOx Films Deposited by Layer-by-Layer Growth for CMOS High-k Gate Dielectrics. Materials Research Society Symposia Proceedings, 2003, 786, 251.	0.1	3
70	High performance PIN Ge photodetector and Si optical modulator with MOS junction for photonics-electronics convergence system. , 2013, , .		3
71	High Density Optical Interconnects Integrated with Lasers, Optical Modulators and Photodetectors on a Single Silicon Chip. , 2013, , .		3
72	A 300mm Si photonics platform for multi-applications. , 2015, , .		3

#	Article	IF	CITATIONS
73	A 300mm Si photonics platform for optical interconnection. , 2015, , .		3
74	Extraction of SOI thickness deviation based on resonant wavelength analysis for silicon photonics devices. , 2017, , .		3
75	High-performance Si optical modulator with strained p-SiGe layer and its application to 25 Gbps optical transceiver. , 2017, , .		3
76	Importance of Leakage Current Noise Analysis for Accurate Lifetime Prediction of High-k Gate Dielectrics. , 2005, , .		3
77	Novel stacked capacitor technology for 1-Gbit DRAMs with (Ba,Sr)TiO3 thin films. Electronics and Communications in Japan, 1997, 80, 70-78.	0.2	2
78	Carrier separation analysis for clarifying leakage mechanism in unstressed and stressed HfAlO/sub x//SiO/sub 2/ stack dielectric layers. , 0, , .		2
79	Vacuum-ultraviolet reflectance difference spectroscopy for characterizing dielectrics–semiconductor interfaces. Thin Solid Films, 2011, 519, 2830-2833.	1.8	2
80	Photonics-Electronics Convergence System for High Density Inter-Chip Interconnects by Using Silicon Photonics. , 2012, , .		2
81	Uniform characteristics of Si-wire waveguide devices fabricated on 300 mm SOI wafers by using ArF immersion lithography. , 2013, , .		2
82	Multi-channel and high-density hybrid integrated light source by thermal management for low power consumption for ultra-high bandwidth optical interconnection. , 2014, , .		2
83	High-performance silicon photonics process platform for low-power photonic integrated circuits. , 2016, , .		2
84	Spectral variation analysis for silicon grating couplers fabricated on a 300-mm SOI wafer. , 2017, , .		2
85	High-density Silicon Optical Interposer for Inter-chip Interconnects based on Compact and High Speed Components. , 2013, , .		2
86	A Compact Monitoring Circuit to Accurately Extract Fabrication Deviation in Silicon Waveguides. , 2020, , .		2
87	Compact behavioral model and parametric extraction for optical phase shifters in carrier-depletion Mach–Zehnder silicon modulators. Optics Communications, 2022, 507, 127645.	2.1	2
88	Understanding Inter-Arm Imbalance in Mach–Zehnder Silicon Optical Modulators: Impact on OMA and Frequency Chirp. Journal of Lightwave Technology, 2022, 40, 5171-5189.	4.6	2
89	Uniformly Aligned Ferroelectric Liquid Crystal Cell Applied to a Light Valve. Molecular Crystals and Liquid Crystals, 1992, 222, 189-194.	0.3	1
90	Integration of Ba x Sr 1-x TiO 3 thin film for DRAM application. , 1995, , .		1

#	Article	IF	CITATIONS
91	Analysis of transient charging components in NBTI degradation studied for TaN gated HfO <inf>2</inf> /SiO <inf>2</inf> dielectrics. , 2007, , .		1
92	High-uniformity waveguide-integrated metal-semiconductor-metal germanium photodetector with sige capping layer and its application to differential receivers. , 2012, , .		1
93	Large-scale silicon photonics integrated circuits for interconnect and telecom applications. , 2013, , .		1
94	Study of Carbonization Process on Surface of Si Substrate in High Vacuum Region with Hydrocarbon Gas. Materials Science Forum, 0, 740-742, 161-164.	0.3	1
95	Growth mechanisms of 3C-SiC layer by carbonization of Si(100) substrates in high-vacuum region. Japanese Journal of Applied Physics, 2014, 53, 045601.	1.5	1
96	Electrical Characterization of 3C-SiC Lateral MOSFETs Fabricated on Heteroepitaxial Films Including High Density of Defects. Materials Science Forum, 2015, 821-823, 733-736.	0.3	1
97	High-performance silicon photonics platform for low-power photonic integrated circuits. , 2017, , .		1
98	Compact modeling and parametric extraction of phase shifters in carrier-depletion Mach-Zehnder silicon modulators. , 2021, , .		1
99	Comparison Studies on Oxygen Diffusion Coefficients for ALD-Al2O3 and PLD-HfO2 Films using 18O Isotope. , 2002, , .		1
100	Advances in High-Density Inter-Chip Interconnects with Photonic Wiring. IEICE Transactions on Electronics, 2013, E96.C, 958-965.	0.6	1
101	Systematic identification of crosstalk and bandwidth upper limit in highly cascaded Mach–Zehnder lattice optical filters. Japanese Journal of Applied Physics, 2022, 61, 022001.	1.5	1
102	Edge enhancement recording with ferroelectric liquid crystal spatial light modulator using SiO2/a-Si:H photosensor. Ferroelectrics, 1993, 149, 207-215.	0.6	0
103	Mechanisms of X-Ray Radiation-Induced Damage in (Ba, Sr)TiO3Capacitors. Japanese Journal of Applied Physics, 1998, 37, 1328-1331.	1.5	0
104	Impact of air-induced poly-Si/oxynitride interface layer degradation on gate-edge leakage. , 2011, , .		0
105	Photonics-Electronics Convergent System Technology. , 2013, , .		Ο
106	First demonstration of athermal silicon optical interposers with quantum dot lasers operating up to 125 °C. , 2014, , .		0
107	Athermal silicon optical interposers with quantum dot lasers operating from 25 to 125°C. Electronics Letters, 2014, 50, 1377-1378.	1.0	0
108	The Influence of the Carbonization Mechanisms on the Crystalline Quality of the Carbonization Layer for Heteroepitaxial Growth of 3C-SiC. Materials Science Forum, 0, 778-780, 230-233.	0.3	0

#	Article	IF	CITATIONS
109	Observation of suppressed dark current of Ge on Si (100) using ultrathin Ge seed layer. , 2014, , .		Ο
110	Low-loss and flatband silicon-nanowire-based 5 <sup>th</sup> -order coupled resonator optical waveguides (CROW) fabricated by ArF-immersion lithography process on a 300-mm SOI wafer. Proceedings of SPIE, 2014, , .	0.8	0
111	Athermal silicon optical interposers operating up to $125 {\hat {\mathsf A}}^{\mathrm o}$ C. Proceedings of SPIE, 2015, , .	0.8	0
112	Ultra-fme Si photonics fabrication technology based on 40-nm-node CMOS process. , 2015, , .		0
113	Spectral variation analysis of integrated silicon photonics devices by using optical wafer probing. , 2018, , .		0
114	Etching yields of HfO2 under Ar+ and CFX+ (X = 1, 2, 3) ion beam irradiation. , 2003, , .		0
115	Degradation Mechanism of HfAlOX/SiO2 Stacked Gate Dielectric Films through Transient and Steady State Leakage Current Analysis. , 2004, , .		0
116	Flat-band Voltage Tunability and No Depletion Effect of Poly-Si Gate CMOS with Nanometer-size Metal Dots at the Poly-Si/Dielectric Interface. , 2004, , .		0
117	Impact of Initial Traps on TDDB and NBTI Reliabilities in High-k Gate Dielectrics. , 2006, , .		0
118	Fully Integrated Silicon Optical Interposers with High Bandwidth Density. , 2014, , .		0
119	Dielectric Properties of (BaxSr1-x)TiO3 Thin Films Deposited by RF Sputtering Hyomen Kagaku, 1996, 17, 660-665.	0.0	0
120	Mechanisms of Synchrotron X-Ray Irradiation-Induced Damage in (Ba,Sr)TiO3 Capacitors. , 1997, , .		0
121	Conformal Step Coverage of (Ba, Sr)TiO3 Films Prepared by Liquid Source CVD Using Ti(t-BuO)2(DPM)2. , 1998, , .		0